Supporting information for

Enhancing remnant polarization in ferroelectric $Hf_{0.5}Zr_{0.5}O_2$ thin films by oxygen-diffusive interlayers

Utaek Cho[1, 2], Joonyong Kim[1, 2, 5], Taegyu Kwon[1, 2, 5], Pyeongkang Hur[3], Daseob Yoon[4], Min Hyuk Park[1, 2, 5, *], and Junwoo Son[1, 2, *]

[1] Department of Materials Science and Engineering, Seoul National University, Seoul 08826, Republic of Korea

[2] Research Institute of Advanced Materials, Seoul National University, Seoul 08826, Republic of Korea

[3] Department of Materials Science and Engineering, Pohang University of Science and Technology (POSTECH), Pohang 37673, Republic of Korea

[4] Department of Electrical Engineering, Display and Semiconductor Engineering, Pukyong National University, Busan 48513, Republic of Korea

[5] Institute of Engineering Research, College of Engineering, Seoul National University, Seoul 08826, Republic of Korea

[*] minhyuk.park@snu.ac.kr

[*] junuson@snu.ac.kr

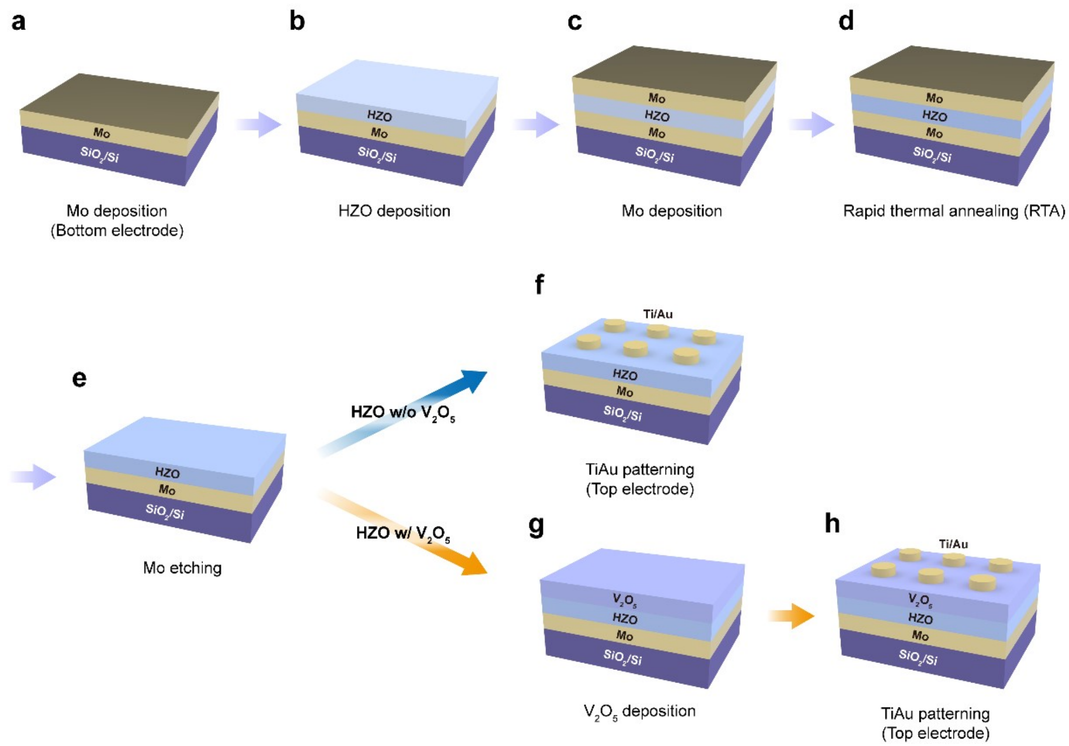

Figure S1 | Schematic fabrication process of HZO capacitors with and without V_2O_5. a, Mo bottom electrode was deposited using a direct current sputtering on bare SiO_2/Si substrate. **b,** HZO was grown using thermal ALD with a substrate temperature of 300 °C. **c,** The Mo top electrode was deposited under the same conditions as the Mo bottom electrode. **d,** The heterostructure of Mo/HZO/Mo/SiO_2/Si was annealed at 500 °C for 30 s using RTP to crystallize HZO film. **e,** Top Mo was etched in an etchant composed of H_3PO_4, HNO_3, CH_3COOH, and DI water. **f,** For HZO without V_2O_5, Ti/Au top electrodes were deposited on HZO using a lift-off process by thermal evaporator. **g,** For V_2O_5/HZO, V_2O_5 layer was deposited on HZO by PLD at 300 °C. **h,** Subsequently, Ti/Au top electrodes were deposited on top of V_2O_5/HZO/Mo/SiO_2/Si structure using the same lift-off process described in **f**. In the fabrication process, HZO layer was intentionally annealed between the Mo electrodes prior to V_2O_5 deposition, aiming to minimize clamping effect induced by the V_2O_5 layer during RTP and to clearly evaluate the intrinsic effect of oxygen diffusion. Detailed experimental conditions are described in the Methods section.

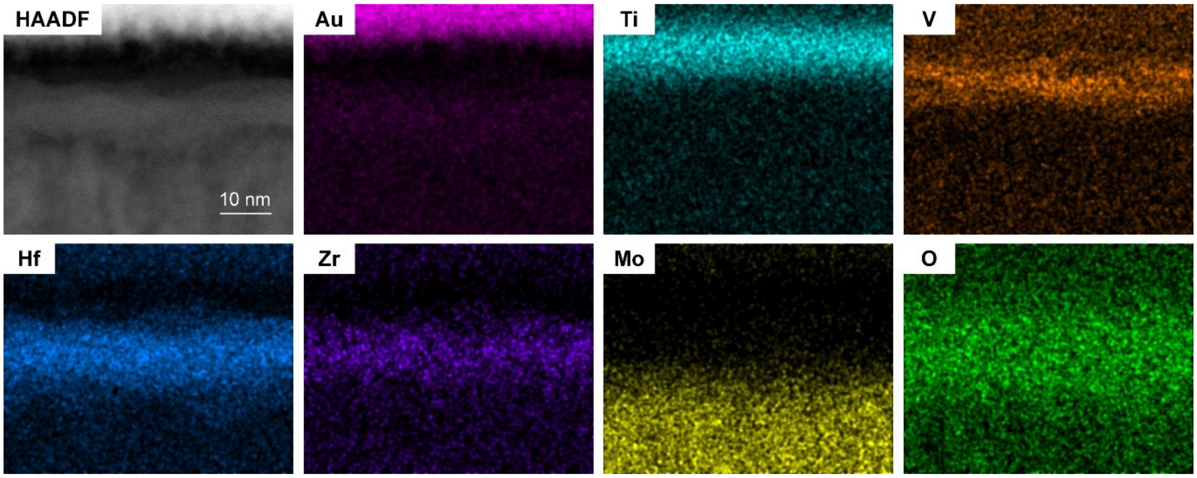

Figure S2 | The cross-sectional STEM image and corresponding EDS mapping of V_2O_5/HZO capacitor with Ti/Au top electrode and Mo bottom electrode. HAADF contrast exhibits a layered structure, as supported by EDS elemental mapping. From top to bottom, Au, Ti, V, (Hf, Zr), and Mo are sequentially distributed, while oxygen is primarily located in the regions excluding the metal electrode.

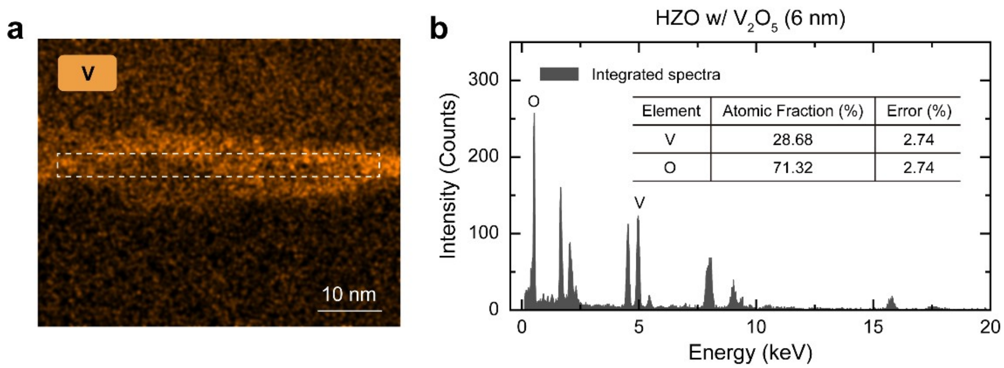

Figure S3 | The cross-sectional EDS analysis of vanadium oxide layer in V_2O_5/HZO capacitor. a, Element mapping of V element, and **b,** average EDS spectrum of vanadium oxide layer. The EDS spectrum was acquired from white dashed box in **a**, confirming that stoichiometric V_2O_5 was formed in vanadium oxide layer (see the inset in **b**).

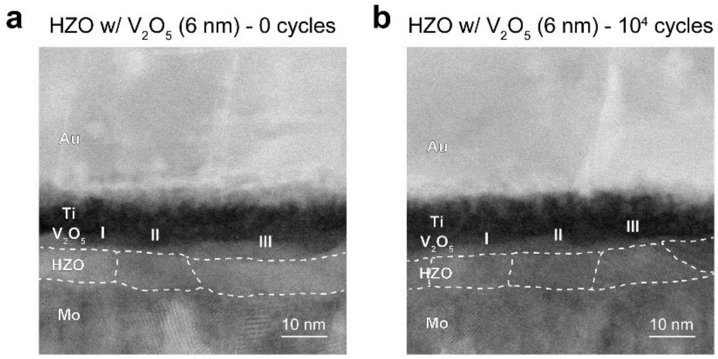

Figure S4 | HAADF images of V_2O_5/HZO capacitors marked with grain boundary. The grain boundaries of the HZO layer are indicated by white dashed lines in the HAADF images of the samples shown in **a,** before wakeup, and **b,** after wakeup of 10^4 cycles.

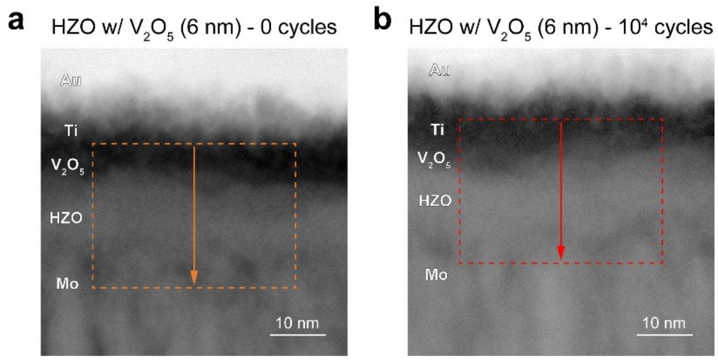

Figure S5 | HAADF images of V_2O_5/HZO capacitors marked with EDS scan range in the vertical direction. Cross-sectional HAADF-STEM images for EDS line profile. The average EDS profile corresponds to the **a,** orange (0 cycles) and **b,** red (10^4 cycles) dashed rectangular area.

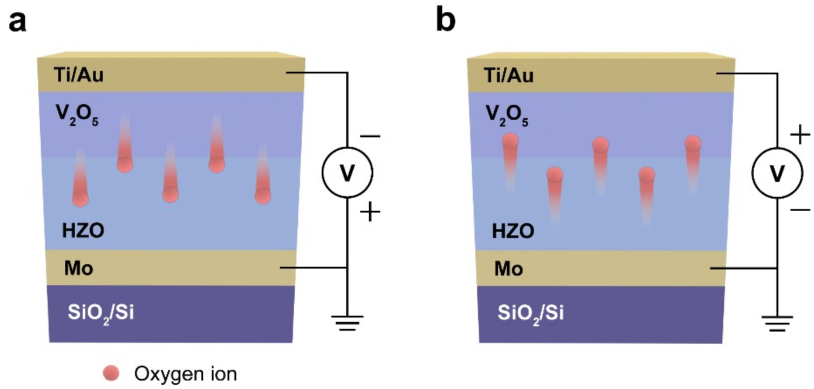

Figure S6 | Schematic of the oxygen ion migration direction in the V_2O_5/HZO capacitor under different bias conditions. a, When a negative voltage is applied to the top electrode, oxygen ions migrate from the V_2O_5 layer toward the HZO layer, leading to the partial reduction of V^{5+} to V^{4+} in V_2O_5 layer. **b,** Conversely, when a positive voltage is applied to the top electrode, oxygen ions drift from the HZO layer toward the V_2O_5 layer, resulting in the re-oxidation of V^{4+} to V^{5+}. Repeated cycling of this process induces the rearrangement of oxygen distribution and the reversible change in the vanadium valence state at the V_2O_5/HZO interface.

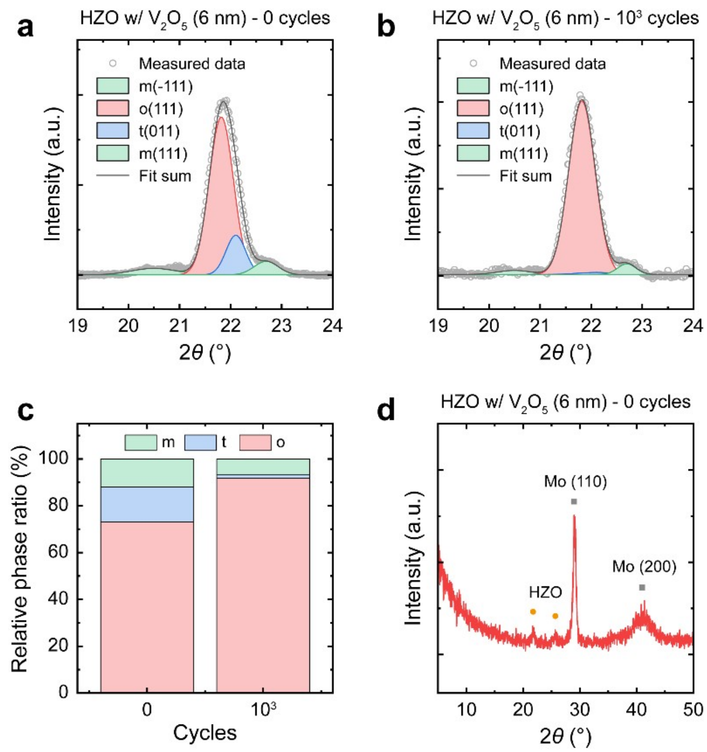

Figure S7 | GIXRD spectra measured before and after wakeup cycles. Deconvoluted GIXRD spectrum of V_2O_5 (6 nm)/HZO with 0 cycles in **a,** and 10^3 cycles in **b**, showing the coexistence of m(-111), m(111), o(111), and t(011) phases. To match the large X-ray beam spot size in grazing incidence geometry, the top electrode was deposited across nearly the entire 2.5 mm × 3.5 mm surface of the sample. **c,** The relative fraction of the o-phase increased from ~73% before wakeup to ~92% after wakeup, while the t-phase almost disappeared. Phase ratios were calculated based on the integrated area of each deconvoluted peak. **d,** The GIXRD scan with a wide 2θ range of 5° ~ 50° in V_2O_5 (6 nm)/HZO with 0 cycles, showing HZO and Mo peaks.

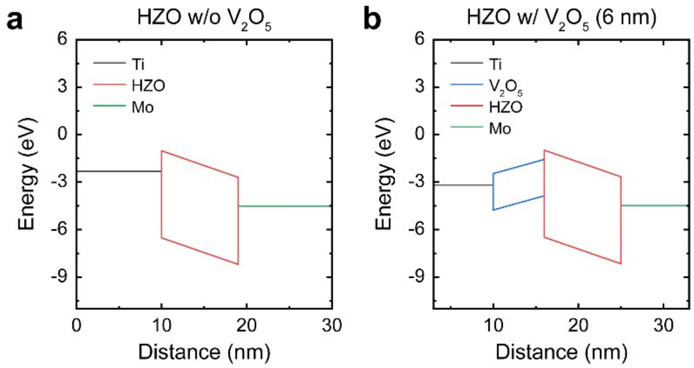

Figure S8 | Schematic energy band diagrams of HZO capacitors. The band diagrams were constructed based on the condition where a negative coercive voltage was applied to HZO capacitors **a,** without and **b,** with the V_2O_5 layer, based on *P–V* curve in **Fig. 1d**. It was assumed that the interfacial charge at V_2O_5/HZO interface corresponds to approximately 70% of the polarization in HZO; This interfacial charge was iteratively calculated to match the voltage drop across the HZO layer at the respective coercive voltages of HZO without V_2O_5 and V_2O_5/HZO capacitors. Under this condition, the voltage drop across HZO layer become identical (= -1.68 V) even though different external voltages were applied, which were -2.2 V for HZO without V_2O_5 and -1.3 V for the HZO with V_2O_5. This result indicates that the insertion of V_2O_5 layer allows HZO film to achieve the large polarization value even at a lower external voltage due to interfacial charge-assisted field enhancement. The material parameters were set as follows: Φ(Ti) = 4.0 eV, Φ(Mo) = 4.52 eV; ε_r(HZO) = 30, E_g(HZO) = 5.5 eV, χ(HZO) = 2.7 eV; ε_r(V_2O_5) = 25, E_g(V_2O_5) = 2.3 eV, and χ(V_2O_5) = 3.28 eV (*Nano Converg.* 10, 55 (2023); *J. Mater. Sci.* 21, 20284-20294 (2021)).